Tubulin Polymerization Promoting Proteins (TPPPs): Members of a New Family with Distinct Structures and Functions†

Orsolya Vincze,[‡,§] Natália Tökési,[‡,§] Judit Oláh,[§] Emma Hlavanda,[§] Ágnes Zotter,[§] István Horváth,[§] Attila Lehotzky,[§] László Tirián,[||] Katalin F. Medzihradszky,[⊥] János Kovács,[#] Ferenc Orosz,[§] and Judit Ovádi*[,§]

Institute of Enzymology, Biological Research Center, Hungarian Academy of Sciences, Budapest, H-1113, Hungary, Department of Biology, Faculty of Medicine, University of Szeged, Szeged, H-6720, Hungary, Department of Pharmaceutical Chemistry, School of Pharmacy, University of California—San Francisco, San Francisco, California 94143-0446, and Department of Anatomy, Cell and Developmental Biology, Faculty of Science, Eötvös Loránd University, Budapest, H-1117, Hungary

Received June 29, 2006; Revised Manuscript Received September 18, 2006

ABSTRACT: TPPP/p25 is a brain-specific protein, which induces tubulin polymerization and microtubule (MT) bundling and is enriched in Lewy bodies characteristic of Parkinson's disease [Tirián et al. (2003) *Proc. Natl. Acad. Sci. U.S.A. 100,* 13976−13981]. We identified two human gene sequences, CG1−38 and p25*β*, which encoded homologous proteins, that we termed p20 and p18, respectively. These homologous proteins display 60% identity with tubulin polymerization promoting protein/p25 (TPPP/p25); however, the N-terminal segment of TPPP/p25 is missing. They could be clustered into three subfamilies present in mammals and other vertebrates. We cloned, isolated, and characterized the structural and functional properties of the recombinant human proteins at molecular, ultrastructural, and cellular levels using a number of tools. These data revealed that, while p20 behaved as a disorganized protein similarly to TPPP/p25, which was described as a flexible and inherently dynamic protein with a long unstructured N-terminal tail, p18 was featured in more ordered fashion. TPPP/p25 and p20 specifically attached to MTs causing MT bundling both *in vitro* and *in vivo*; p18 protein did not cross-link MTs, and it distributed homogeneously within the cytosol of the transfected HeLa cells. These data indicate that the two shorter homologues display distinct structural features that determine their associations to MTs. The properties of p20 resemble TPPP/p25. The bundling activity of these two proteins results in the stabilization of the microtubular network, which is likely related to their physiological functions.

Recently, we have isolated a heat-stable protein from bovine brain, named tubulin polymerization promoting protein/p25 (TPPP/p25),[1] the major intracellular target of which is the microtubular system (*1*, *2*). Our data including *in silico* analysis showed that TPPP/p25, with its low α-helix content, belongs to the group of intrinsically unstructured proteins that have been extensively studied in the last years (*3*−*6*). Structural studies with human recombinant protein suggest that this protein, indeed, displays a flexible, unusual secondary structure involving folded structural elements (*7*).

We have shown that TPPP/p25 isolated from bovine brain promotes tubulin polymerization into double-walled tubules and polymorphic aggregates at a substoichiometric concentration; its binding to paclitaxel-stabilized microtubules (MTs) induces bundling as judged by electron and atomic force microscopies (*1*, *8*). TPPP/p25 co-localizes selectively with the microtubular system in eukaryotic cells causing stabilization of the network; the overexpression of this protein in transfected HeLa cells induces a characteristic protein aggregation (aggresome formation) (*2*). We have proposed that this latter process could be related to the enrichment of TPPP/p25 in inclusion bodies of the pathological human brain. Indeed, TPPP/p25 showed complete co-localization with α-synuclein in the Lewy bodies in the case of Parkinson's disease and other synucleinopathies (*6*, *9*, *10*).

As we described previously, TPPP/p25 is the first member of a new protein family, the primary sequence of which differs from that of other known proteins, but shows high homology with p25-like hypothetical proteins sought via BLAST (*8*). In the human genome, there are two gene sequences that are homologous with that of TPPP/p25: CG1−38 and p25*β*, which encode proteins that we termed p20 (176 amino acids) and p18 (170 amino acids), respectively. The genes of TPPP/p25, p20, and p18 are located on the 5th, 16th, and 14th chromosomes, respectively (*11*, *12*). Recently, we have reported that the TPPP/p25 gene is

† This work was supported by Hungarian National Scientific Research Fund Grants OTKA T-046071 and TS-044730 to J. Ovádi and T-049247 to F.O. and by FP6-2003-LIFESCIHEALTH-I, Bio-Sim, NKFP-MediChem2 1/A/005/2004 to J. Ovádi K.F.M. was supported by NIH Grants NCRR RR001614 and NCRR RR012961 to the UCSF Mass Spectrometry Facility.

* To whom correspondence should be addressed: Institute of Enzymology, Biological Research Center, Hungarian Academy of Sciences, Budapest, Karolina út 29, H-1113, Hungary. Telephone: (36-1) 279-3129. Fax: (36-1) 466-5465. E-mail: ovadi@enzim.hu.

‡ The first two authors contributed equally to this work.

§ Hungarian Academy of Sciences.

|| University of Szeged.

⊥ University of California—San Francisco.

Eötvös Loránd University.

[1] Abbreviations: DSC, differential scanning calorimetry; MT, microtubule; TPPP/p25, tubulin polymerization promoting protein/p25; CD, circular dichroism; SPR, surface plasmon resonance; TEM, transmission electron microscopy; EGFP, enhanced green-fluorescent protein.

10.1021/bi061305e CCC: $33.50
Published on Web 11/01/2006

conserved in the genomes of ciliated organisms but is absent from those that are nonciliated, suggesting crucial involvement for TPPP/p25 in the superstructure of basal bodies/centrosomes (*13*). The distribution of this protein was tested in various tissues using mono- and polyclonal antibodies, and it was detected exclusively in the brain (*14*). Takahasi et al. reported that the TPPP/p25 expression at the protein level increased with age in rat brain (*15*).

CGI-38 gene, an evolutionarily conserved gene of *Caenorhabditis elegans* was found in the human genome by comparative genomic searching (*16*). Its orthologue was also identified in the mouse transcriptome (RIKEN cDNA 2700055K07) (*17*). Here, we present evidence that the p20 protein is expressed in bovine brain tissue. Human p18 was found at the mRNA level and cloned from a fetal brain cDNA library by Zhang et al. (*12*). They demonstrated that it was highly expressed in the liver and pancreas and had a moderate expression level in the heart, skeletal muscle, and kidney. The transcript was not detected in the lung, placenta, or brain, except in fetal brain.

In this paper, we introduce this new family, the TPPPs, by characterizing their structural and functional properties at molecular, ultrastructural, and cellular levels. We suggest that the disordered structures of TPPP/p25 and p20 from this family could determine their MT-related, probably physiological functions.

MATERIALS AND METHODS

DNA Manipulation. HexaHis-tagged TPPP/p25 was cloned and expressed in *Escherichia coli* as described elsewhere (*9*, *10*); p18 and p20 cDNA clones (IMAGE ID: 5169309 and 3349849, respectively (*17*); see also http://image.lln-l.gov/) were obtained from MRC Geneservice. The open-reading frames were amplified with the following primers, containing *Xho*I and *Nhe*I restriction sites for the 5′ end and *Eco*RI restriction site for the 3′ end: P18fw, AGTTCTCGAGCTAGCATGGCATCAGAGGCAGAAA; P18rev, TTATGAATTCTACTTGGTCTTCTTATC; and P20fw, AGTTCTCGAGCTAGCATGGCAGCGAGCACAGA; P20rev, TTATGAATTCACTTCTTCACCTTGGCA. For the generation of bacterial expression vectors producing HexaHis-tagged p18 and p20 proteins (pTrcHisp18 and pTrcHisp20), the polymerase chain reaction (PCR) products were cloned between *Nhe*I and *Eco*RI sites into the pTrcHisB expression vector (Stratagene). For DsRed2 fusion protein expression in mammalian cells (pDsRed2p18 and pDsRed2p20), the PCR products were cloned between *Xho*I and *Eco*RI sites into the pDsRed2C1 expression vector (Clontech). The polycloning sites and the inserted open-reading frames of the recombinant vectors were verified by sequencing.

Identification of Bovine Brain p20. p20 was co-purified from bovine brain with TPPP/p25 as described previously (*1*). An approximately 20 kDa protein isolated and sodium dodecyl sulfate−polyacrylamide gel electrophoresis (SDS−PAGE)-purified was in-gel-digested with trypsin following our protocol (http://donatello.ucsf.edu/ingel.html). The digest of peptides was analyzed by LC/MS/MS. The fractionation was carried out using an Ultimate-nanoHPLC system using a PepMap 75 μm ID column as described previously (*18*). The eluant was analyzed using a Pulsar, quadrupole-orthogonal-acceleration time-of-flight hybrid tandem mass spectrometer (MD Sciex, Toronto, Canada). Database searches were performed using the Mascot search engine (www.matrixscience.com).

Prediction of Unstructured Regions. Sequences were submitted to the PONDR server (http://www.pondr.com) using the default integrated predictor VL-XT (*19*, *20*). Access to PONDR was provided by Molecular Kinetics (IUETC, Indianapolis, IN; e-mail: main@molecularkinetics.com) under the license from the WSU Research Foundation.

Protein Determination. The protein concentration was measured by the Bradford method (*21*) using the Bio-Rad protein assay kit.

Tubulin and MT Preparation. Tubulin purified from bovine brain by the method of Na and Timasheff (*22*) was assembled to MTs as described previously (*1*).

Limited Proteolysis. A total of 2 mg/mL of TPPP/p25, p20, or p18 was digested with 0.01 mg/mL trypsin IV (kindly provided by Prof. L. Gráf from the Eötvös Loránd University, Budapest, Hungary) in 50 mM Tris buffer (pH 8.0) containing 10 mM $CaCl_2$ at 25 °C. A control experiment was performed under the same conditions, except that the trypsin was omitted. Aliquots were drawn from each sample at different time points. The digestion was terminated by the addition of protease inhibitor, 4-(2-aminoethyl)benzenesulphonyl fluoride, solution in 1 mM final concentration. The samples were analyzed on tricine−SDS−PAGE gels. The assay for chymotrypsin (Sigma) proteolysis was that 1 mg/mL TPPPs was digested with 0.005 mg/mL chymotrypsin in 50 mM 2-(*N*-morpholino)ethanesulfonic acid buffer (pH 7.0) containing 5 mM $CaCl_2$, 1 mM ethylene glycol bis(2-aminoethyl ether)-*N*,*N*,*N*′,*N*′-tetraacetic acid (EGTA), and 1 mM $MgCl_2$ at 25 °C.

Circular Dichroism (CD) Measurements. CD spectra were acquired with a Jasco J-720 spectropolarimeter (Tokyo, Japan) in the 190−260 nm wavelength range employing 0.1 cm thermostated cuvettes at 25 °C, using 10 mM phosphate buffer (pH 7.0). Scanning was repeated 3 times, and the spectra were averaged. The difference spectrum was obtained by subtracting the spectra of the individual proteins from the measured spectrum of the mixture of two proteins (tubulin plus TPPP/p25, p20, or p18).

Surface Plasmon Resonance (SPR). The binding kinetics of TPPP/p25 and its homologues to tubulin were monitored in real time with a BIAcore X instrument (BIAcore). The TPPP/p25 homologues were immobilized onto the nickel−nitrilotriacetic acid (Ni−NTA) chip through their His tags. The running buffer was 0.01 M 4-(2-hydroxyethyl)-1-piperazineethanesulfonic acid (pH 7.4), containing 0.15 M NaCl, 50 μM ethylenediaminetetraacetic acid, and 0.005% P20 detergent. Tubulin was injected into the immobilized protein surface in various concentrations for 2 min at a flow rate of 5 μL/min. Bound tubulin was removed from the chip with a 1 min pulse of 2 M NaCl solution. The thermodynamic and kinetic parameters were obtained by fitting the sensorgrams with the Langmuir 1:1 binding model using the BiaEvaluation 3.0 software (BIAcore).

Differential Scanning Calorimetry (DSC). DSC studies were conducted on a MicroCal VP-DSC calorimeter (MicroCal, Northhampton, MA). The cell volume was 0.5 mL; the rate of heating was 1 °C/min; and the excess pressure was kept equal to 49 psi. Thermograms for lysozyme, TPPP/p25, p20, and p18 were recorded in 25 mM phosphate buffer

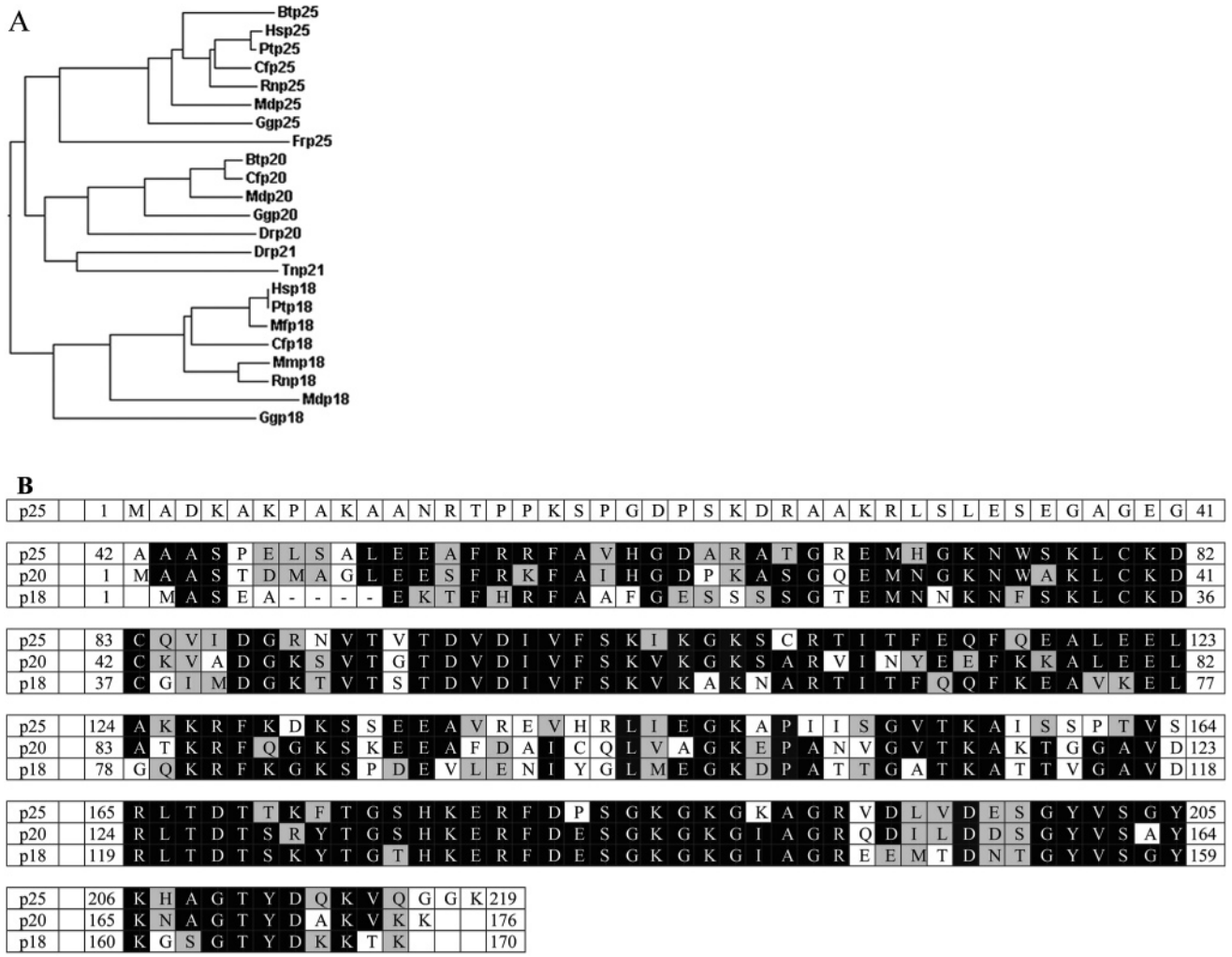

FIGURE 1: (A) Phylogenetic tree of the vertebrate TPPP/p25 family. The multiple alignment of the sequences and the tree was produced by ClustalW (*28*). Bt, *Bos taurus*; Hs, *Homo sapiens*; Pt, *Pan troglydes*; Mf, *Macaca fascicularis*; Cf, *Canis familiaris*; Mm, *Mus musculus*; Rn, *Rattus norvegicus*; Md, *Monodelphis domestica*; Gg, *Gallus gallus*; Fr, *Fugu rubripes*; Dr, *Danio rerio*; and Tn, *Tetraodon nigroviridis*. Drp21 and Tnp21 mark 178 amino acid homologues found only in fish [some of the homologues (Mm p25, Tn p25, Hs p20, Mm p20, Rn p20, and Bt p18) are not shown for the clarity of the figure]. (B) Multiple alignment of the human TPPP/p25 and its homologues. Identical and similar residues are indicated by black and gray backgrounds, respectively.

(pH 7.0), and the protein concentrations were between 10 and 40 μg/mL. The thermogram of buffer was subtracted, and each thermogram was normalized using the concentration of the corresponding protein. The calorimetric enthalpy change (ΔH_{cal}) was calculated by integrating the area in each heat capacity curve.

Transmission Electron Microscopy (TEM). Tubulin was assembled to MTs as described previously (*1*). MTs were incubated with 0.5 mg/mL TPPP/p25 or its homologues. After 30 min, the sample was centrifuged at 30000*g* and 30 °C for 20 min and the pellet fraction was used for TEM. Samples for electron microscopic studies were prepared as described in Tirián et al. (*8*).

Cell Culture, Manipulation, Immunostaining, and Fluorescent Microscopy. HeLa (ATCC, CCL-2) cells were grown as described in Lehotzky et al. (*2*). Transfections with pEGFP/p25, pDsRed2-p20, or pDsRed2-p18 were carried out with Fugene6 reagent (Roche) according to the instructions of the manufacturer. Cells were treated with 50 nM vinblastine (Sigma) for 2 h at the end of the transfection period (24 h). Cells were fixed with cold methanol and immunostained for α-tubulin (DMA-1 monoclonal, Sigma), followed by Texas-Red/fluorescein isothiocyanate-conjugated anti-mouse antibody (Jackson Laboratories), all diluted in 5% fetal calf serum−phosphate-buffered saline (PBS) buffer. Nuclei were counterstained with 4′,6-diamidino-2-phenylindole. Images were recorded on a Leica DMLS epifluorescent microscope and were processed by Adobe Photoshop. We counted a sum of 434 transfected cells in 15 microscopic fields from three independent transfection experiments to evaluate the percentage distribution of the different ultrastructures induced by TPPP/p25 expression. We used an Apofluor objective with 40× magnification. Samples were exposed with the same time (25 s).

RESULTS

Phylogenetic Tree and Structural Predictions. The primary sequence of TPPP/p25 differs from that of other proteins known thus far; however, it shows a high degree of homology with p25-like hypothetical proteins (*8*). Our search using BLAST (*23*) has shown that such proteins can be found throughout the animal kingdom (and in the green algae) but not in prokaryotes, land plants, or fungi, etc. As the phylogenetic tree shows (Figure 1A), in vertebrates, they can

be clustered into three subgroups according to TPPP/p25, p20, and p18. These subfamilies seem to be present only in mammals (human, chimpanzee, bovine, rat, mouse, dog, and opossum) and other vertebrates (chicken and fish).

In the cases of the members of the p20 and p18 subfamilies, however, the N-terminal region of TPPP/p25, i.e., the first 40−42 amino acids, is missing. The sequence comparison of the three (hypothetical) proteins (Figure 1B) shows 53% identity. The pairwise comparisons of similarities are 81, 76, and 75% for p25−p20, p20−p18, and p25−p18, respectively. These data suggest that the highest similarity is between TPPP/p25 and p20 (apart from the missing N-terminal part). Considering all of the vertebrate homologues, the phylogenetic tree also indicates a close relationship between the TPPP/p25-like and p20-like proteins (cf. Figure 1). It is worth noting that the similarities of the paralogues are comparable with that found between the orthologues, e.g., between human and Fugu fish TPPP/p25 (79%).

A neural network-based algorithm, PONDR, was developed to search disordered regions of proteins (*19*, *20*). Now, we have predicted the disordered and ordered regions of the homologues by this approach that has been successfully used in a prediction study for TPPP/p25 (*6*). The disordered regions of TPPP/p25 appear to be the most extended as compared to those of the two shorter forms (Figure 2). Quantitative evaluation of the prediction data presented in Table 1 unambiguously indicates the distinct conformation state of TPPPs even if the disordered N-terminal segment is disregarded. The overall percent of disorder is substantially higher for TPPP/p25 and p20 than for p18; the disordered regions of TPPP/p25 and p20 are similar to each other and significantly longer than that of p18. Therefore, the amino acid substitution(s) in p20 and p18 may result in structural alterations.

Proof of p20 Protein Expression. An approximately 20 kDa protein (p20) was found in a partially purified fraction of TPPP/p25 isolated from bovine brain. The final step of the TPPP/p25 isolation, as we described previously (*1*), is a salt-gradient elution from a cation-exchange column. The fraction eluting at a lower salt concentration than TPPP/p25 contains an approximately 20 kDa protein estimated by its SDS−PAGE mobility (data not shown). This band was cut from the gel and in-gel-digested with trypsin. Collision-induced dissociation data acquired in an LC/MS/MS analysis of the tryptic digest identified sequences: FAIGDPK, AVTGTDVDIVFSK, VINYEEFK, VINYEEFKK, SKEEAFDAICQLVAGK, QDILDDSGYVSAYK, and <QDILDDSGYVSAYK (<Q stands for pyroglutamic acid), corresponding to hypothetical bovine protein AAI02516 [gi:73587319] (a homologue of human and mouse CGI-38 hypothetical proteins, NP_057048 and NP_080757, respectively) predicted tryptic peptides (17−24), (49−61), (69−76), (69−77), (91−106), and (152−165), respectively (mascot scores ranged from 32 to 98). These peptides represent 35% of the protein sequence.

Distinct Structures of TPPPs. Proteolysis is a sensitive method to test the structural integrity of proteins (*24*). Trypsin IV, a human brain-specific protease (*25*), and chymotrypsin were used to test the conformational features of the homologues (Figure 3). The SDS−PAGE images of the time-dependent proteolysis of the three proteins showed that (i) TPPP/p25 is degraded after 2 h, (ii) the shorter proteins display less vulnerability toward both proteases, (iii) the shorter homologues feature stable bands even after 2 h of incubation, and (iv) the p18 seems to be the most folded protein, because in the case of trypsin IV digestion, a significant fraction of this protein remains intact after 2 h (Figure 3) and even after 4 h of digestion (data not shown). These data reveal that the structural integrity of TPPP/p25 (if there is any) is much lower than that of the shorter homologues, especially that of p18, and that the desintegrity is not restricted to the N-terminal segment of TPPP/p25 but that protease-sensitive bonds are exposed in additional parts of the protein as well.

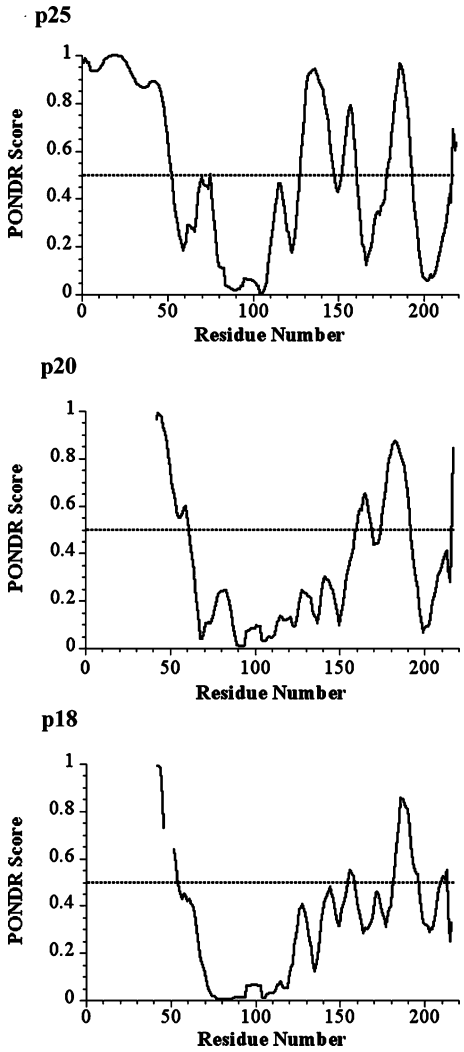

FIGURE 2: PONDR predictions of structural order/disorder of TPPP/p25 and its homologues. Disorder prediction values (PONDR scores) of a given residue are plotted against the residue number. Only the residue numbers of TPPP/p25 are shown to make the plots comparable. The significance threshold, above which residues are considered to be disordered, set to 0.5, is shown.

The unfolding of proteins by elevation of the temperature is accompanied by a positive heat capacity change, which can be quantified by DSC. We used this approach to obtain comparative data for the temperature-induced structural alterations in the cases of TPPP/p25, p20, and p18. The measurements and the evaluation of the data were validated using a well-established globular protein, lysozyme (*26*). In Figure 4A, typical DSC thermograms of the homologous proteins together with that of lysozyme are presented.

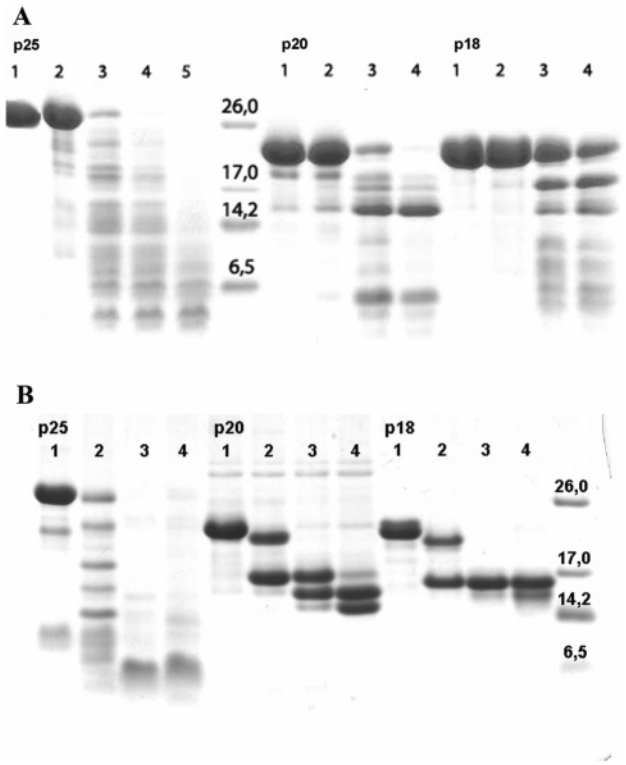

FIGURE 3: (A) Time-dependent limited proteolysis of TPPP/p25, p20, and p18 with trypsin IV. Lane 1, native proteins without protease; and lanes 2−5, digest patterns after 0, 30, 60, and 120 min, respectively. (B) Time-dependent limited proteolysis of TPPP/p25, p20, and p18 with chymotrypsin. Lane 1, native proteins without protease; and lanes 2−4, digest patterns after 0, 30, and 120 min, respectively.

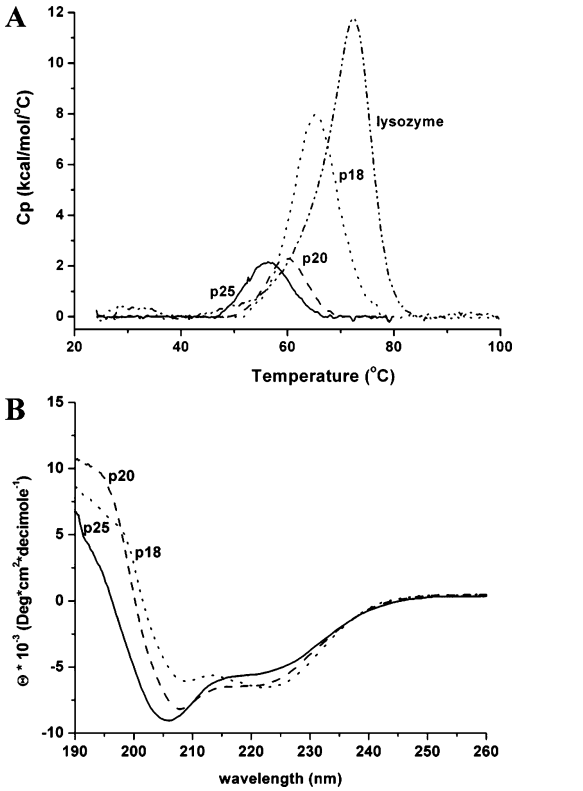

FIGURE 4: (A) Normalized thermograms of TPPP/p25, p20, and p18 obtained by DSC. Thermograms of TPPP/p25 (—), p20 (- - -), p18 (···), and lysozyme (-···-) were recorded in 25 mM phosphate buffer (pH 7.0). For other details, see the Materials and Methods. (B) Normalized far-UV CD spectra of TPPP/p25 (—), p20 (- - -), and p18 (···).

Lysozyme behaves in our system as expected, displaying the transition temperature (T_m) at 72.1 ± 0.1 °C (*26*). Concerning the features of the homologues, there are significant differences in their molar heat capacity functions as shown in Table 1. T_m values for TPPP/p25 and p20 are similar and significantly lower as compared to that for p18. The calorimetric enthalpy change (ΔH_{cal}) is associated with the disruption of intramolecular interactions and the concomitant formation of interactions between water and unburied groups because of the unfolding process. The ΔH_{cal} values of all TPPPs evaluated are much lower than that for lysozyme. The values for TPPP/p25 and p20 are similar to each other but lower than that of p18. Significant temperature-induced structural alterations occur only in p18. These data indicate that the stabilizing elements are missing or occur at a very low level in the cases of these two homologues.

The CD spectra of the human recombinant homologues, TPPP/p25, p20, and p18, were measured in the far-UV range to obtain comparative data for the secondary structures of TPPPs. Figure 4B shows that the spectrum of TPPP/p25 is characteristic of unfolded proteins, and it is similar to that obtained with TPPP/p25 isolated from bovine brain (*1*). The comparative analysis of the CD spectra elucidates differences in the secondary structures of the TPPPs, and p18 displays a CD spectrum characteristic of folded proteins.

Different Association with Tubulin. To test whether the structural differences manifest themselves in the association of the TPPPs with tubulin, CD and SPR measurements were performed.

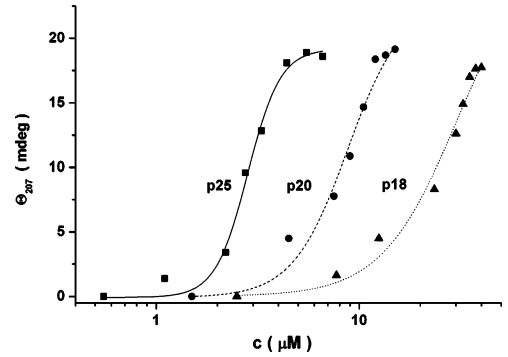

FIGURE 5: Difference ellipticity of 1 μM tubulin and the homologues at 207 nm as a function of the concentration of TPPP/p25 (■), p20 (●), and p18 (▲). Difference ellipticities were calculated from the ellipticity determined at 207 nm in the mixtures of two proteins and in the samples of the individual proteins.

The addition of tubulin to the homologues resulted in a positive difference in the ellipticity spectra in the cases of all three proteins, indicating that they interact with tubulin (data not shown) and that the interaction causes significant enhancement in the secondary structure of the partner proteins. The titration curves of the three homologues with tubulin based on the difference ellipticity at 207 nm (Figure 5) show significant differences in their binding affinities to tubulin (cf. Table 2).

SPR is a sensitive method to quantify the elementary steps of the association/dissociation processes of protein−protein interactions. By means of this approach, we characterized the association of tubulin to the TPPPs. The kinetic param-

Table 2: Kinetic and Thermodynamic Parameters of the Interactions between TPPP/p25, p20, p18, and Tubulin[a]

	SPR			CD
	k_{on} (M^{-1} s^{-1}) $\times 10^3$	k_{off} (s^{-1}) $\times 10^{-3}$	K_D (M) $\times 10^{-6}$	EC_{50} (M)
TPPP/p25 (human)	7.7 ± 0.7	2.5 ± 0.1	0.32 ± 0.03	2.5×10^{-6}
p20	4.5 ± 0.5	4.5 ± 0.2	1.0 ± 0.1	8×10^{-6}
p18	2.3 ± 0.1	5.8 ± 0.1	2.5 ± 0.1	25×10^{-6}

[a] The k_{on}, k_{off}, and K_D parameters were determined by SPR, and the EC_{50} values were based on the difference ellipticity evaluated from the CD measurements.

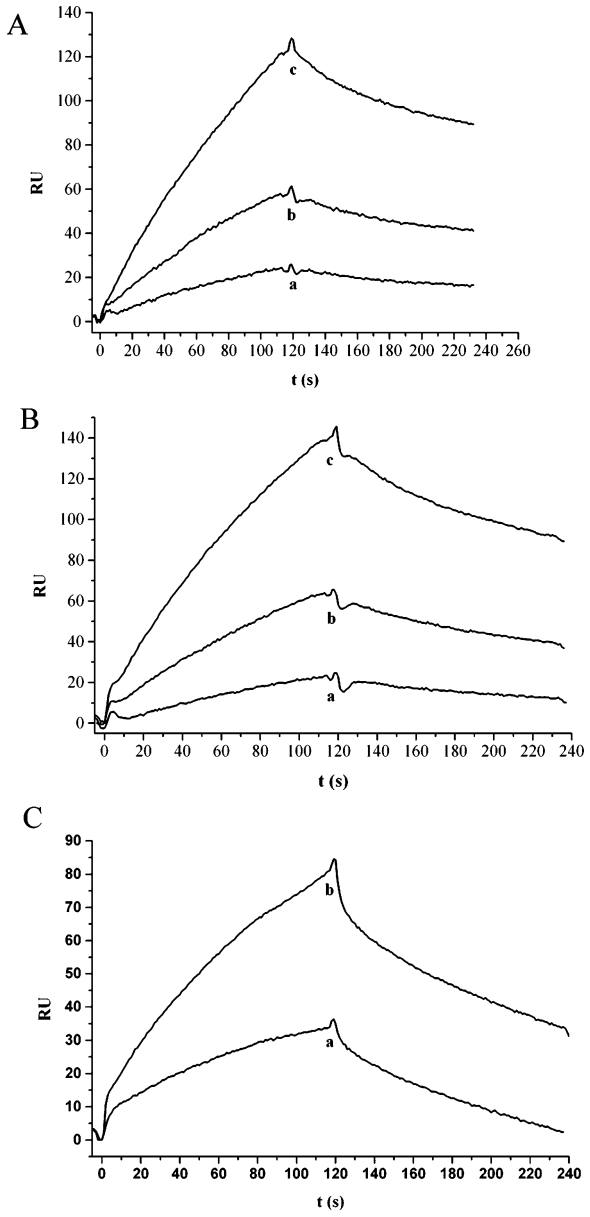

FIGURE 6: SPR studies of the interactions of the immobilized homologues with tubulin. In all cases, 900 response units of His-tagged protein (A, TPPP/p25; B, p20; and C, p18) were immobilized onto the Ni−NTA groups on the chip surface. Sensorgrams were obtained with 0.25 μM (a), 0.5 μM (b), and 1 μM (c) tubulin for TPPP/p25, with 0.5 μM (a), 1 μM (b), and 2 μM (c) tubulin for p20, and with 1 μM (a) and 2 μM (b) tubulin for p18, respectively.

eters were evaluated from the sensorgrams obtained with the homologues at three different tubulin concentrations (Figure 6). The association/dissociation rate and affinity constants (k_{on}, k_{off}, and K_D) of the interactions of TPPP/p25, p20, or p18 with tubulin are summarized in Table 2. These results are in agreement with that obtained by CD measurements, showing that TPPP/p25 and p18 has the highest and lowest affinity to tubulin, respectively.

TPPP/p25 and p20 Induce MT Bundling. Pelleting experiments suggested that TPPP/p25 and p20 proteins bind to MTs (data not shown). The consequences of these heteroassociations on the MT ultrastructure were investigated by TEM studies that were performed. The control samples contained only taxol-stabilized MTs, which were long, loosely arranged single MTs of about 25 nm in diameter (Figure 7A). In sharp contrast, MTs form large bundles of closely aligned MTs in the presence of TPPP/p25 (Figure 7B). Surprisingly, p20 shows even higher bundling activity, and apparently, all of the MTs form a large bundled but not amorphous mass in the pellet (Figure 7C). The MTs in the p18-treated samples are similar to that of the control, suggesting that this protein lacks any bundling activity on MTs (Figure 7D).

The intracellular localization and bundling activity of TPPP/p25 was investigated in transiently transfected HeLa cells. At a low expression level, TPPP/p25 is aligned with the microtubular network, without causing ultrastructural or morphological alterations (*2*). A total of 24% of the transfected cells showed this clear alignment with the microtubular network. At a high expression level, the fusion protein induces significant morphological alterations; two distinct structures are formed: aggresome-like body (cell marked 1 in Figure 8A) or perinuclear cage (cell marked 2 in Figure 8A), with the co-localization of tubulin and TPPP/p25 (*2*). The percentage distribution of the highly transfected cells containing aggresome-like body, cage, and not well-defined ultastructures showed the following ratio: 41, 21, and 38%, respectively.

In HeLa cells transfected with pDsRed2-p20 or pDsRed2-p18, the red-fluorescent signal was visualized by epifluorescence microscopy. Protein p20 induces extensive bundling of the microtubular network, and bundled MTs are mostly accumulated around the nucleus (Figure 8C). Virtually, the perinuclear bundles seemed to be thicker in the pDsRed2-p20-transfected cells than the nuclear cage observed in TPPP/p25-expressing cells (cf. Figure 8A, cell marked 2, and Figure 8C, and also see ref *2*). Moreover, in the case of p20, the bundled cytoplasmic filaments are curved and turn back from the periphery of the cell, which is an unusual behavior of MTs. The expression of p20 was able to rearrange the normal, axial ultrastructure of MTs into a concentric one around the nucleus. A total of 60% of the transfected cells showed this characteristic feature. The rest (40%) exhibited bundled MTs but not perinuclear arrangement.

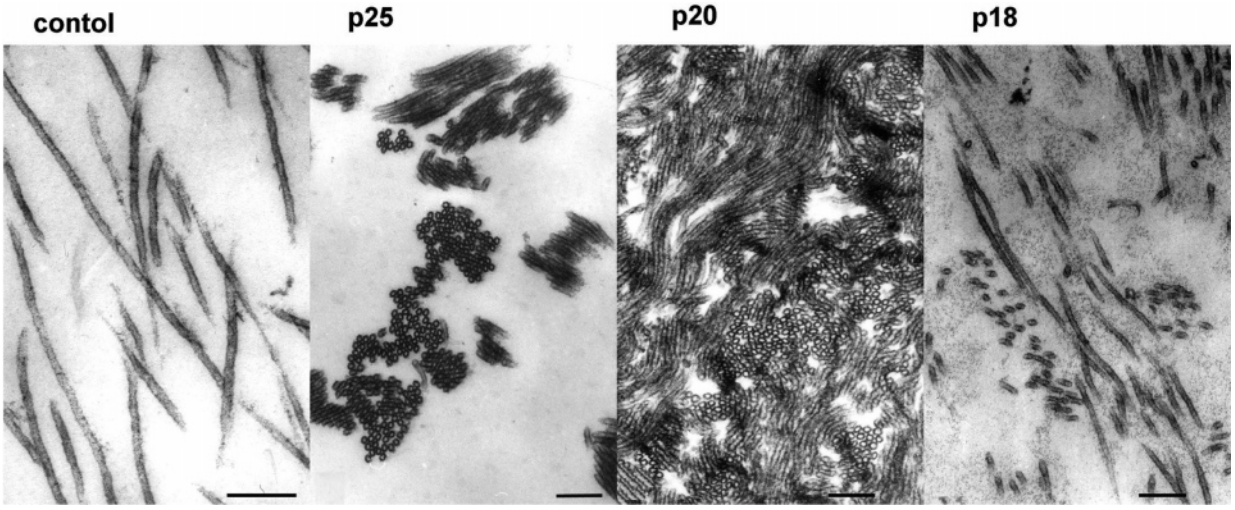

FIGURE 7: Electron microscopic analysis of the effect of TPPP/p25, p20, and p18 on MTs prepared as described in the Materials and Methods. Loosely arranged, long MTs are seen in the control sample prepared in the absence of the homologoues. Both TPPP/p25 and p20 induce the formation of large MT bundles, which are absent in samples prepared with p18. Bars = 150 nm.

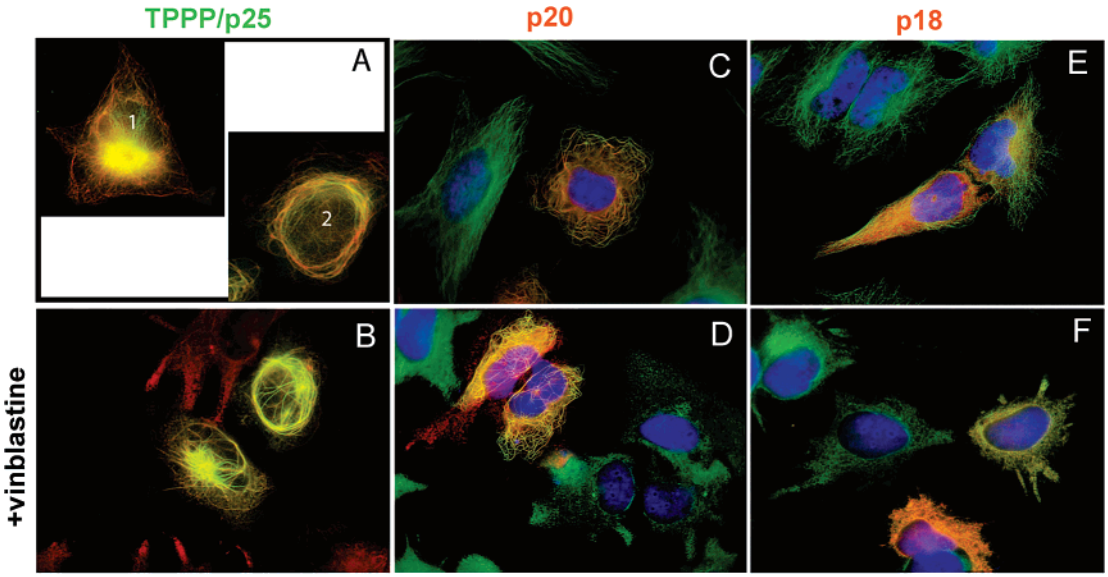

FIGURE 8: Fluorescence images of HeLa cells transfected with pEGFP-TPPP/p25 (A and B), pDsRed-p20 (C and D), and pDsRed-p18 (E and F). Tubulin was detected by immunocytochemistry (red, A and B; and green, C−F). Note the ultrastructures induced by TPPP/p25: aggresome-like body and perinuclear cage (A, cell marked 1 and 2, respectively) and induced by p20: the meandering filaments surround the nucleus (C) in contrast to the homogeneous cytoplasmatic distribution of p18 (E). Co-localization of the MTs with TPPP/p25 and p20 (orange in A−D) but not with p18 (E and F) is visible. Pictures of B, D, and F show the effect of vinblastine (50 nM) treatment in the last 2 h of the transfection period. In the nontransfected cells, the MT network is completely dissolved in the cytoplasm, but in cells transfected with TPPP/p25 (B) or p20 (D), the bundled microtubular fibers are preserved.

In contrast to the co-localization of TPPP/p25 and p20 with the MTs, p18 apparently displays homogeneous cytoplasmic distribution (Figure 8E).

To see whether the TPPPs affect the stability of MT structures, cells were treated with vinblastine, a specific MT-destabilizing agent. The microtubular network was completely collapsed in the untransfected cells, and the depolymerized MTs (stained by Texas-Red or fluorescein isothiocyanate-conjugated antibodies) were homogenously distributed in the cytosol (cf. Figure 8B, D, F). In the transfected cells, although a fraction of the green-fluorescent TPPP/p25 was detached from the microtubular network, the bundled MTs were still decorated by enhanced green-fluorescent protein (EGFP)−TPPP/p25. This observation that TPPP/p25 counteracts the effect of vinblastine is in agreement with our previous findings (*2*). We demonstrated that the resistance of MTs bundled by p20 against vinblastine was even more pronounced compared with TPPP/p25; the antimicrotubular agent did not affect the bundled microtubular ultrastructure (cf. Figure 8D); i.e., virtually no diffuse signal of tubulin was visualized. Similar qualitative images were observed when the transfected cells were treated with 0.4 μM nocodazole, another antimicrotubular agent, in 30 min of the last period of the 24 h transfection (data not shown). Therefore, the stabilizing effect of p20 on the microtubular network is likely due to its extensive bundling activity. p18 did not exert any protective effect on the microtubular network, the transfected and the nontransfected cells did not show any difference in terms of morphology, and the green signal of tubulin distributed diffusely in the cells (Figure 8F).

Table 1: Predicted and Experimental Structural and Stability Data of TPPP/p25 and Its Human Homologues

		prediction of disorder by PONDR			experimental data from		
					DSC		CD
	number of amino acids	number of disordered amino acids	overall percent disordered	longest disordered region	T_m (°C)	ΔH_{cal} (kcal/mol)	Θ_{205} (mdeg cm^2 dmol^{-1})
TPPP/p25	219	100	45.66	52 amino acids	56.4 ± 0.1	21 ± 2	−8.9
TPPP/p25 without N-terminal tail[a]	165	53	31.12	20 amino acids			
p20	176	47	26.70	20 amino acids	59.7 ± 0.1	21 ± 2	−8.0
p18	170	31	18.24	15 amino acids	65.1 ± 0.1	85 ± 5	−5.7

[a] The C-terminal part of TPPP/p25 homologues is known as the Pfam05517 domain (the 55−219 amino acids in TPPP/p25; see ref *29* and http://www.sanger.ac.uk/Software/Pfam).

DISCUSSION

In this work, we identified and characterized proteins of a new protein family, which are encoded by different genes of the human genome and display high sequence homology, apart from the N-terminal tail of TPPP/p25. The TPPPs showed significant differences in their structural features; while TPPP/p25 is a flexible and inherently dynamic protein, protein p18 rather than p20 shows a stable structure as revealed by the physical characterization of these proteins (cf. Table 1). In fact, p20 behaves as a disorganized protein similar to TPPP/p25, while p18 behaves in a more ordered fashion. Thus, these distinct features cannot be attributed exclusively to the presence of the N-terminal region of TPPP/p25 because it is missing from both p20 and p18.

Concerning the bindings of these proteins to tubulin, we found a clear affinity order: TPPP/p25 > p20 > p18 based on the CD and SPR data. The K_D value of TPPP/p25 is lower with 1 order of magnitude than that of p18. A recent study demonstrated that a truncated version of TPPP/p25 (termed Δ3-43p25α) behaved as the full-length protein, suggesting that the unstructured N-terminal segment does not play a significant, if any, role in tubulin binding (*7*). Rather, the amino acid substitutions in the C-terminal parts of the homologues could be crucial from this respect. Such small but crucial differences may result in the missing or very low level of stabilizing elements, such as helicity, burial of the hydrophobic surface area, and tight packing in the hydrophobic core.

Indeed, these characteristics are key factors concerning the ability of unstructured proteins to enter in macromolecular associations (*3*). Our data suggest that the MTs are potent interacting partners for TPPP/p25 and p20 both *in vitro* and *in vivo*. The binding constants of these proteins are comparable with that of MAP2c or tau proteins, which are in the micromolar range (*27*). The heteroassociations of TPPP/p25 and p20, similar to MAPs, lead to significant ultrastructural alterations of the microtubular network. We demonstrated by TEM and immunofluorescence microscopy using isolated proteins and transfected HeLa cells, respectively, that the MTs were extensively bundled by TPPP/p25 and p20 proteins but not by p18, causing an extensive increase in the stability of MTs. Structural changes of these flexible, unfolded proteins could be induced by their heteroassociations with tubulin/MTs, which can increase their life span against proteolytic degradation.

It is an important question whether the N-terminal segment of TPPP/p25 has any physiological/pathological function. It does not appear to be directly involved in MT binding; however, its regulatory role even in the tubulin-related function cannot be excluded. Nevertheless, it is reasonable to assume that it might have a pro-aggregatory role in the formation of pathological inclusions. The evaluation of this assumption was motivated by our recent observations, namely, that the formation of the aggresome-like body was produced in HeLa cells exclusively by overexpression of TPPP/p25 (cf. Figure 8) but not by p20. Because extensive enrichment of TPPP/p25 was found in pathological inclusions (*9*), the aggresome formation at the cell level might mimic the pathological situation. Further studies are needed to prove this hypothesis and to clarify whether the protein p20 is involved in any pathological process.

REFERENCES

1. Hlavanda, E., Kovács, J., Oláh, J., Orosz, F., Medzihradszky, K. F., and Ovádi, J. (2002) Brain-specific p25 protein binds to tubulin and microtubules and induces aberrant microtubule assemblies at substoichiometric concentrations, *Biochemistry 41*, 8657−8664.
2. Lehotzky, A., Tirián, L., Tökési, N., Lénárt, P., Szabó, B., Kovács, J., and Ovádi, J. (2004) Dynamic targeting of microtubules by TPPP/p25 affects cell survival, *J. Cell Sci. 117*, 6249−6259.
3. Dunker, A. K., Brown, C. J., Lawson, J. D., Iakoucheva, L. M., and Obradovic, Z. (2002) Intrinsic disorder and protein function, *Biochemistry 41*, 6573−6582.
4. Wright, P. E., and Dyson, H. J. (1999) Intrinsically unstructured proteins: Re-assessing the protein structure−function paradigm, *J. Mol. Biol. 293*, 321−331.
5. Uversky, V. N. (2002) What does it mean to be natively unfolded? *Eur. J. Biochem. 269*, 2−12.
6. Orosz, F., Kovács, G. G., Lehotzky, A., Oláh, J., Vincze, O., and Ovádi, J. (2004) TPPP/p25: From unfolded protein to misfolding disease: Prediction and experiments, *Biol. Cell 96*, 701−711.
7. Otzen, D. E., Lundvig, D. M., Wimmer, R., Nielsen, L. H., Pedersen, J. R., and Jensen, P. H. (2005) p25α is flexible but natively folded and binds tubulin with oligomeric stoichiometry, *Protein Sci. 14*, 1396−1409.
8. Tirián, L., Hlavanda, E., Oláh, J., Horváth, I., Orosz, F., Szabó, B., Kovács, J., Szabad, J., and Ovádi, J. (2003) TPPP/p25 promotes tubulin assemblies and blocks mitotic spindle formation, *Proc. Natl. Acad. Sci. U.S.A. 100*, 13976−13981.
9. Kovács, G. G., László, L., Kovács, J., Jensen, P. H., Lindersson, E., Botond, G., Molnár, T., Perczel, A., Hudecz, F., Mezö, G., Erdei, A., Tirián, L., Lehotzky, A., Gelpi, E., Budka, H., and Ovádi, J. (2004) Natively unfolded tubulin polymerization promoting protein TPPP/p25 is a common marker of α-synucleinopathies, *Neurobiol. Dis. 17*, 155−162.
10. Lindersson, E., Lundvig, D., Petersen, C., Madsen, P., Nyengaard, J. R., Hojrup, P., Moos, T., Otzen, D., Gai, W. P., Blumbergs, P. C., and Jensen, P. H. (2004) p25α stimulates α-synuclein aggregation and is co-localized with aggregated α-synuclein in α-synucleinopathies, *J. Biol. Chem. 280*, 5703−5715.
11. Seki, N., Hattori, A., Sugano, S., Suzuki, Y., Nakagawara, A., Muramatsu, M., Hori, T., and Saito, T. (1999) A novel human

gene whose product shares significant homology with the bovine brain-specific protein p25 on chromosome 5p15.3, *J. Hum. Genet. 44*, 121−122.
12. Zhang, Z., Wu, C., Huang, W., Wang, S., Zhao, E., Huang, Q., Xie, Y., and Mao, Y. (2002) A novel human gene whose product shares homology with bovine brain-specific protein p25 is expressed in fetal brain but not in adult brain, *J. Hum. Genet. 47*, 266−268.
13. Ovádi, J., Orosz, F., and Lehotzky, A. (2005) What is the biological significance of the brain-specific tubulin-polymerization promoting protein (TPPP/p25)? *IUBMB Life 57*, 765−768.
14. Takahashi, M., Tomizawa, K., Ishiguro, K., Sato, K., Omori, A., Sato, S., Shiratsuchi, A., Uchida, T., and Imahori, K. (1991) A novel brain-specific 25 kDa protein (p25) is phosphorylated by a Ser/Thr-Pro kinase (TPK II) from tau protein kinase fractions, *FEBS Lett. 289*, 37−43.
15. Takahashi, M., Tomizawa, K., Fujita, S. C., Sato, K., Uchida, T., and Imahori, K. (1993) A brain-specific protein p25 is localized and associated with oligodendrocytes, neuropil, and fiber-like structures of the CA hippocampal region in the rat brain, *J. Neurochem. 60*, 228−235.
16. Lai, C. H., Chou, C. Y., Ch'ang, L. Y., Liu, C. S., and Lin, W. (2000) Identification of novel human genes evolutionarily conserved in *Caenorhabditis elegans* by comparative proteomics, *Genome Res. 10*, 703−713.
17. Strausberg, R. L., Feingold, E. A., Grouse, L. H., Derge, J. G., Klausner, R. D., Collins, F. S., Wagner, L., Shenmen, C. M., Schuler, G. D., Altschul, S. F., Zeeberg, B., Buetow, K. H., Schaefer, C. F., Bhat, N. K., Hopkins, R. F., Jordan, H., Moore, T., Max, S. I., Wang, J., Hsieh, F., Diatchenko, L., Marusina, K., Farmer, A. A., Rubin, G. M., Hong, L., Stapleton, M., Soares, M. B., Bonaldo, M. F., Casavant, T. L., Scheetz, T. E., Brownstein, M. J., Usdin, T. B., Toshiyuki, S., Carninci, P., Prange, C., Raha, S. S., Loquellano, N. A., Peters, G. J., Abramson, R. D., Mullahy, S. J., Bosak, S. A., McEwan, P. J., McKernan, K. J., Malek, J. A., Gunaratne, P. H., Richards, S., Worley, K. C., Hale, S., Garcia, A. M., Gay, L. J., Hulyk, S. W., Villalon, D. K., Muzny, D. M., Sodergren, E. J., Lu, X., Gibbs, R. A., Fahey, J., Helton, E., Ketteman, M., Madan, A., Rodrigues, S., Sanchez, A., Whiting, M., Madan, A., Young, A. C., Shevchenko, Y., Bouffard, G. G., Blakesley, R. W., Touchman, J. W., Green, E. D., Dickson, M. C., Rodriguez, A. C., Grimwood, J., Schmutz, J., Myers, R. M., Butterfield, Y. S., Krzywinski, M. I., Skalska, U., Smailus, D. E., Schnerch, A., Schein, J. E., Jones, S. J., and Marra, M. A. (2002) Generation and initial analysis of more than 15,000 full-length human and mouse cDNA sequences, *Proc. Natl. Acad. Sci. U.S.A. 99*, 16899−16903.
18. Medzihradszky, K. F. (2005) In-solution digestion of proteins for mass spectrometry, *Methods Enzymol. 405*, 50−65.
19. Li, X., Romero, P., Rani, M., Dunker, A. K., and Obradovic, Z. (1999) Predicting protein disorder for N-, C-, and internal regions, *Genome Inf. 10*, 30−40.
20. Romero, P., Obradovic, Z., Li, X., Garner, E. C., Brown, C. J., and Dunker, A. K. (2001) Sequence complexity of disordered protein, *Proteins 42*, 38−48.
21. Bradford, M. M. (1976) A rapid and sensitive method for the quantitation of microgram quantities of protein utilizing the principle of protein−dye binding, *Anal. Biochem. 72*, 248−254.
22. Na, C. N., and Timasheff, S. N. (1986) Interaction of vinblastine with calf brain tubulin: Multiple equilibria, *Biochemistry 25*, 6214−6222.
23. Altschul, S. F., Madden, T. L., Schäffer, A. A., Zhang, J., Zhang, Z., Miller, W., and Lipman, D. J. (1997) Gapped BLAST and PSI-BLAST: A new generation of protein database search programs, *Nucleic Acids Res. 25*, 3389−3402.
24. Tsai, C. J., Polverino de Laureto, P., Fontana, A., and Nussinov, R. (2002) Comparison of protein fragments identified by limited proteolysis and by computational cutting of proteins, *Protein Sci. 11*, 1753−1770.
25. Katona, G., Berglund, G. I., Hajdú, J., Gráf, L., and Szilágyi, L. (2002) Crystal structure reveals basis for the inhibitor resistance of human brain trypsin, *J. Mol. Biol. 315*, 1209−1218.
26. Privalov, P. L., Tiktopulo, E. I., Venyaminov, S. Y., Griko, Y. V., Makhatadze, G. I., and Khechinashvili, N. N. (1989) Heat capacity and conformation of proteins in the denatured state, *J. Mol. Biol. 205*, 737−750.
27. Felgner, H., Frank, R., Biernat, J., Mandelkow, E. M., Mandelkow, E., Ludin, B., Matus, A., and Schliwa, M. (1997) Domains of neuronal microtubule-associated proteins and flexural rigidity of microtubules, *J. Cell. Biol. 138*, 1067−1075.
28. Thompson, J. D., Higgins, D. G., and Gibson, T. J. (1994) CLUSTAL W: Improving the sensitivity of progressive multiple sequence alignment through sequence weighting, position-specific gap penalties and weight matrix choice, *Nucleic Acids Res. 22*, 4673−4680.
29. Bateman, A., Coin, L., Durbin, R., Finn, R. D., Hollich, V., Griffiths-Jones, S., Khanna, A., Marshall, M., Moxon, S., Sonnhammer, E. L., Studholme, D. J., Yeats, C., and Eddy, S. R. (2004) The Pfam protein families database, *Nucleic Acids Res. 32*, D138−D141.

BI061305E